AAC Accepted Manuscript Posted Online 10 April 2017
Antimicrob. Agents Chemother. doi:10.1128/AAC.00443-17

Title: Synthetic (p)ppGpp analogue: Inhibitor of stringent response in mycobacteria

Kirtimaan Syal,[1] Kelly Flentie,[2] Neerupma Bhardwaj,[1] Krishnagopal Maiti,[3] Narayanaswamy Jayaraman,[3] Christina L. Stallings,[2] and Dipankar Chatterji[1*]

1. Molecular Biophysics Unit, Division of Biological Sciences, Indian Institute of Science, Bangalore, India 560012
2. Department of Molecular Microbiology, Washington University School of Medicine, Campus Box 8230, 660 S. Euclid Avenue St. Louis, MO 63110 USA
3. Department of Organic Chemistry, Division of Chemical Sciences, Indian Institute of Science, Bangalore, India 560012

Correspondence:

E. mail- dipankar@mbu.iisc.ernet.in

Phone- +91 80 22932836

Fax- +91 80 23600535

Short Running Title: *Stress Response Inhibitor of Mycobacteria*

Contribution

KS carried out the experiments. KF carried out the work on *M. tuberculosis* biofilms and reproduced *M. smegmatis* biofilm work. NB did permeability and MTT toxicity assay. KF and NB contributed equally. KGM and NJ helped in the synthesis and in NMR based characterization of compounds. CS designed the work on Mtb and partly wrote the paper. KS and DC designed the experiments and wrote the paper.

Abstract

Bacteria elicit an adaptive response against hostile conditions such as starvation and other kind of stresses. Their ability to survive such conditions depends on, in part, stringent response pathways. (p)ppGpp, considered to be the master regulator of stringent response, is a novel target for inhibiting the survival of the bacteria. In mycobacteria, the (p)ppGpp synthetase activity of bifunctional Rel is critical for its stress response and persistence inside the host. Our aim was to design an inhibitor of (p)ppGpp synthesis, follow efficiency through enzyme kinetics, and assess its phenotypic effects in mycobacteria. As such, new sets of inhibitors targeting (p)ppGpp synthesis were synthesized and characterized by mass spectrometry and NMR spectroscopy. We observed significant inhibition of (p)ppGpp synthesis by Rel_{Msm} in the presence of designed inhibitors in a dose dependent manner, which we further confirmed by following the enzyme kinetics. The Rel enzyme-inhibitor binding kinetics were investigated by isothermal titration calorimetry. Subsequently, the effects of the compounds on long term persistence, biofilm formation and biofilm disruption were assayed in *Mycobacterium smegmatis*, where inhibition in each case was observed. *In-vivo* (p)ppGpp levels were found to be down-regulated in *M. smegmatis* treated with the synthetic inhibitors. Compounds reported here also inhibited biofilm formation by the pathogen *Mycobacterium tuberculosis*. The compounds were tested for toxicity by MTT assay using H460 cells and hemolysis assay using Human RBCs, for which they were found to be non-toxic. The permeability of compounds across the cell membrane of human lung epithelial cells was also confirmed by mass spectrometry.

Introduction

Under stress, bacteria generate a response known as "Stringent Response", to enhance their resilience in stressful and nutrient limited conditions. This involves the production and accumulation of an altered nucleic acid base (Guanosine pentaphospahte or Guanosine tetraphosphate, collectively called (p)ppGpp). It is now known that (p)ppGpp has a substantial role in regulation of many physiological processes including transcription, translation, replication, GTP homeostasis, viability and virulence (1-4). In *B. subtilis*, a (p)ppGpp null mutant failed to survive in non-stressed conditions due to dysregulated GTP homeostasis (5).

Mycobacterium tuberculosis, the causative agent of tuberculosis (TB), is the major pathogen responsible for human mortality in the world. Successful treatment of TB requires administration of multiple drugs for at least six months. The major reason for this prolonged treatment of TB is the bacterium's ability to survive under a dormant state, which makes it tolerant to various inhibitors used in the treatment regimen.

In mycobacteria, (p)ppGpp is synthesized and degraded by the bifunctional Rel protein, encoded by the *rel* gene. When this gene was deleted in *M. smegmatis* and *M. tuberculosis,* the knockout strains (Δ*rel*) lost their long-term survival ability during nutrition starvation (6-7). Additionally, the Δ*rel* strain of *M. tuberculosis* was unable to persist in mice (8) and unable to form tubercle lesions in guinea pigs (9), demonstrating the importance of (p)ppGpp in virulence. Specifically, the synthetase activity of the bifunctional Rel has been shown to be critical for the persistence of *M. tuberculosis* in mice (10). Many studies indicate that mycobacteria lacking (p)ppGpp are defective in biofilm formation and antibiotic tolerance (10-12). Most antibiotics target cellular components like ribosomes and cell wall, mainly affecting the bacterial metabolism.

But, bacteria can adjust their metabolism to survive in different conditions, including entering a state of dormancy. So, there is a need to develop new inhibitor compounds to target the 'alternate adaption strategies' of dormant bacteria (11). The stringent response is an attractive target with this goal in mind.

Active research is searching for compounds that can inhibit the synthesis of (p)ppGpp by Rel enzyme. Recently, a molecule named Relacin has been synthesized for inhibiting (p)ppGpp formation. It was designed based on the Rel/Spo (from *S. equisimilis*) crystal structure, where a 2′-deoxyguanosine-based analogue of alarmone molecule ppGpp with the original pyrophosphate moieties at positions 5′ and 3′ replaced by glycyl-glycine dipeptides (13-14). Docking studies were carried out in which Relacin was modeled onto the Rel/SpoT synthetase site. A range of hydrogen bonds/hydrophobic interactions and occupation of the site was taken into consideration, thereby providing a structural basis for the inhibitory effect of Relacin (13-14) (Figure 1). However, the efficiency of these analogues is not appreciable. It has been reported that the isobutyryl group at C-2 of guanine base in Relacin molecule is critical for inhibition. Therefore, we decided to synthesize a more potent compound by functionalization of the amine group at C-2 position of the guanine base in Relacin.

<Figure 1>

97 **Material and Methods**

98 **Synthesis**

99 All chemicals were purchased from Sigma Aldrich and were used without further
100 purification. Solvents were dried and distilled before use. Silica gel (100–200 and 230-
101 400 mesh) was used for column chromatography and TLC analysis was performed on
102 commercial plates coated with silica gel 60 F_{254}. Visualization of the spots on TLC
103 plates was achieved by UV radiation or spraying 5% sulfuric acid in ethanol. High
104 resolution mass spectra were obtained from Q-TOF instrument by electrospray
105 ionization (ESI) and MALDI-TOF. ^{1}H and ^{13}C NMR spectral analyses were performed
106 on a spectrometer operating at 400 MHz and 100 MHz, respectively. Chemical shifts
107 are reported with respect to tetramethylsilane (TMS) for ^{1}H NMR and the central line
108 (77.0 ppm) of $CDCl_3$ for ^{13}C NMR spectroscopy. Coupling constants (*J*) are reported in
109 Hz. Standard abbreviations s, d, t, dd, br s, m refer to singlet, doublet, triplet, doublet of
110 doublet, broad singlet, multiplet.

111

112 ***a.*** ***N*^{2},2',3',5'-*O*-Tetraacetylguanosine (1)**

113 Acetic anhydride (0.4 mL, 4.24 mmol) and 4-dimethylamino pyridine (0.009 g, 0.071
114 mmol) were added to a suspension of guanosine (0.2 g, 0.71 mmol) in pyridine (2 mL)
115 at 0 ^{o}C, stirred for 12 h at room temperature.The reaction mixture was diluted with
116 CH_2Cl_2 (40 mL), washed with dil. aq. HCl (2 x 10 mL), satd. aq. $NaHCO_3$ (1 x 10 mL)
117 and brine (10 mL), dried (Na_2SO_4), filtered and concentrated *in vacuo* and purified
118 (SiO_2) (EtOAc) to afford **1**(0.18 g, 56%);^{1}H NMR ($CDCl_3$, 400 MHz) δ 12.15 (br s, 1
119 H), 10.47 (s, 1 H), 7.77 (s, 1 H), 5.90-5.86 (m, 2H), 5.54 (t, *J* = 4.5Hz, 1 H), 4.42 (dd, *J*
120 = 4.5 Hz, 11.6 Hz, 1 H), 4.33 (dd, *J* = 4.8 Hz, 10 Hz, 1 H), 4.23 (dd, *J* = 5.8 Hz, 11.6
121 Hz, 1 H), 2.25 (s, 3 H), 2.04 (s, 3 H), 2.00 (s, 3 H), 1.99 (s, 3 H); ^{13}C NMR ($CDCl_3$, 100

MHz) δ 172.9, 170.9, 169.6, 169.4, 155.6, 147.9, 138.4, 121.8, 87.2, 79.8, 72.6, 70.6, 63.0, 24.1, 20.6, 20.4, 20.2; HRMS (ESI/TOF-Q) *m/z*: calcd. for $C_{18}H_{21}N_5O_9Na$ = 474.1237, found 474.1236 $[M + Na]^+$, 925.2655 $[2M + Na]^+$.

b. ***N*^{2},2'-*O*,3'-*O*,5'-*O*-Tetrabenzoylguanosine (2)**

Benzoyl chloride (0.98 mL, 8.5 mmol) and DMAP (0.017 g, 0.14 mmol) was added to a suspended solution of guanosine (0.4 g, 1.41 mmol) in pyridine (3 mL) at 0 ^oC, stirred for 12 h at room temperature. The reaction mixture was diluted with CH_2Cl_2 (60 mL), washed with dil. aq. HCl (2 x 20 mL), satd. aq. $NaHCO_3$ (1 x 20 mL) and brine (20 mL), dried (Na_2SO_4), filtered and concentrated *in-vacuo* and purified (SiO_2) (pet. ether:EtOAc = 1:1) to afford **2** (0.62 g, 62%); ^1H NMR ($CDCl_3$, 400 MHz) δ 11.94 (br s, 1 H), 9.53 (s, 1H), 8.15 (d, *J* = 7.6 Hz, 2 H), 7.97 (d, *J* = 6.8 Hz, 4 H), 7.84 (s, 1 H), 7.73 (d, *J* = 7.2 Hz, 2 H), 7.69 (d, *J* = 7.2 Hz, 1 H), 7.59 (t, *J* = 7.8 Hz, 4 H), 7.52-7.47 (m, 1 H), 7.44 (d, *J* = 8 Hz, 2 H), 7.40 (d, *J* = 8 Hz, 2 H), 7.23 (d, *J* = 7.6 Hz, 2 H), 6.92 (dd, *J* = 5.2 Hz, 7.6 Hz, 1 H), 6.45 (dd, *J* = 2 Hz, 5.2 Hz, 1 H), 6.18 (d, *J* = 2 Hz, 1 H), 4.89-4.83 (m, 2 H), 4.78-4.74 (m, 1 H); ^{13}C NMR ($CDCl_3$, 100 MHz) δ 167.3, 166.3, 166.0, 165.1, 155.2, 147.5, 139.0, 133.9, 133.8, 133.6, 131.6, 129.8, 129.7, 129.2, 129.0, 128.8, 128.7, 128.6, 128.5, 128.4, 128.3, 128.0, 122.3, 88.0, 79.3, 74.2, 70.7, 61.5; ESI-MS *m/z*: calcd. for $C_{38}H_{29}N_5O_9Na$ = 722.1863 $[M + Na]^+$, found 722.1865.

c. **N^2-Benzoyl-2',3',5'-*O*-triacetylguanosine (3)**

Aq. NaOH (2 M) (0.1 mL) was added to a solution of **2** (0.3 g, 0.43 mmol) in MeOH (2 mL), stirred for 12 h at room temperature, neutralised with amberlite ion (H^+) exchange resin, filtered and concentrated *in vacuo*. Acetic anhydride (0.19 mL, 2.05mmol) and4-dimethylamino pyridine (0.005 g, 0.041 mmol) were added to the resulting product

147 (0.16 g, 0.41 mmol) in pyridine (2 mL) at 0 °C, stirred for 12 h at room temperature.
148 The reaction mixture was diluted with CH_2Cl_2 (40 mL), washed with dil. aq. HCl (2 x
149 10 mL), satd. aq. $NaHCO_3$ (1 x 10 mL) and brine (10 mL), dried (Na_2SO_4), filtered and
150 concentrated *in vacuo* and purified (SiO_2) (pet. ether:EtOAc= 2:3) to afford **3**(0.09 g,
151 41%, after two steps);^{1}H NMR ($CDCl_3$, 400 MHz) δ 12.2 (br s, 1 H), 9.46 (br s, 1 H),
152 8.02 (d, *J* = 8 Hz, 2 H), 7.72 (br s, 1 H), 7.59 (t, *J* = 7.3 Hz, 1 H), 7.48 (t, *J*= 7.3 Hz, 2
153 H), 5.99-5.87 (m, 3 H), 4.47 (dd, *J* = 3.4 Hz, 11.5 Hz, 1 H), 4.43-4.39 (m, 1 H), 4.35
154 (dd, *J* = 5.6 Hz, 11.5 Hz, 1 H), 2.10 (s, 3 H), 2.05 (s, 3 H), 1.97 (s, 3 H); ^{13}C NMR
155 ($CDCl_3$, 100 MHz) δ 171.0, 169.9, 167.8, 155.4, 147.9, 133.8, 131.3, 129.0, 127.9,
156 87.2, 79.5, 72.9, 70.7, 62.8, 20.7, 20.6, 20.4; HRMS (ESI/TOF-Q)*m/z*: calcd. for
157 $C_{23}H_{23}N_5O_9Na$ = 536.1393, found 536.1392 $[M + Na]^+$, 1049.3358 $[2M + Na]^+$.
158 The acetylated compound and acetylated benzoylated compound were soluble in
159 water up to 1 mg/mL and 0.4 mg/mL, respectively. Both compounds were obtained as
160 white powder.
161
162 **Isothermal Titration Calorimetry**
163 ITC analysis was conducted on the ITC200 Micro Calorimeter (manufactured
164 by GE Healthcare). The Rel enzyme (protein) was added into the cell component (200
165 µl) and syringe (40µl) was filled by the acetylated benzoylated (AB) compound
166 (ligand). Protein was quantified using Bradford assay. Protein and ligand were prepared
167 in the same buffer (20 mM TrisCl pH 7.9 and 50 mM NaCl). Protein concentration
168 varying from 5 µM to 40 µM and ligand concentration varying from 125 µM to 700 µM
169 were used in all experiments. Data obtained were fitted using single binding site model
170 by Origin software (Version 7.0, MicroCal). The first data point was deleted and the
171 ligand-buffer control accounting for heat of dilution (of ligand) was subtracted. Peak

integration and calculation of stoichiometry/Ka/other parameters were also done in Origin software. Experiments were reproduced at least three times.

Activity assay

pET 21b plasmid containing Rel cassette was employed for Rel protein preparation. *E. coli* DH5α and *E. coli* BL21 (DE3) strains were utilized for plasmid purification, protein overexpression and purification, respectively. The identity of protein and its purity was confirmed by SDS-PAGE analysis followed by mass spectrometry (15). For tracing the pppGpp synthesis, (γ)-$^{-}P^{32}$-ATP (125 µCi, 3500 Ci $mmol^{-1}$) was added to the assay mixture containing 200 µg of purified Rel full length protein, 1 mM non-radioactive ATP, 50 mM HEPES (pH 7.4), 5 mM $MgCl_2$, 50 mM NaCl and 1mM GTP in a reduced condition as described previously (16-18). The compounds were added to the reaction mixture at zero time point. The protein was precipitated by heating at 95°C for 5 min and subsequently reaction mixture was subjected to centrifugation at 14000 rpm. The supernatant was loaded on a polyethyleneimine (PEI) cellulose sheet for Thin Layer Chromatography (TLC) analysis followed by phosphor-imaging (BIORAD-PharosFX Plus Molecular Imager). The pppGpp spot was analyzed by densitometric analysis using Image J software (available at the website of National Institute of Health, USA) and the levels of pppGpp were determined.

Enzyme kinetics

Rel from *M. smegmatis* is a bifunctional protein with both (p)ppGpp synthesis and hydrolysis activities. We quantified the synthesis activity of the enzyme in the presence of synthetic compounds. The V_{max} and $K_{0.5}$ values were derived from the steady state kinetic experiments for the full-length Rel protein. The radioactive pppGpp spots were

197 quantified as described previously and the standard curve was plotted (12, 19). The
198 kinetic parameters such as $K_{0.5}$ and V_{max} were calculated using Hill equation. The
199 pppGpp synthesis assay was carried out by using a range of substrate (GTP)
200 concentrations in order to follow the enzyme kinetics. The substrate (GTP)
201 concentration range of 0 to 3000 μM was employed for acetylated benzoylated (AB)
202 compound, whereas in case of control and acetylated (AC) compound, substrate
203 concentration was varied from 0 to 2000 μM. The range was adjusted to achieve
204 saturation. $K_{0.5}$ and V_{max} values derived from the enzyme kinetics in the presence of
205 compounds were compared to the values obtained from enzyme kinetics in the absence
206 of compounds. Assay mixture without enzyme was taken as the negative control.
207

208 ***In-vivo* quantification assay for (p)ppGpp synthesis**

209 *M. smegmatis* mc^2155 strain was cultured in the presence of AB and AC compounds to
210 an OD_{600} of 0.2 in 5 ml 1× MOPS defined medium supplemented with 80 μg/ml
211 Casamino acids, 0.05% Tween 80, 2% glucose at 37°C with agitation. Cultures were
212 radiolabeled by adding [*o*-^{32}P]phosphoric acid (specific activity, >3,000 mCi/mmol;
213 BRIT) directly to the growth medium to a final concentration of 100 μCi/ml. Cells were
214 harvested at 72 h of growth followed by lyophilization. Equal amount of cells were
215 suspended in 20 μl of 1X MOPS solution. Cells were lysed by addition of 12 N formic
216 acid, and stored on ice for 20 min. Sample was subjected to centrifugation at 13,000
217 rpm, 4°C, for 10 min. 2 μl of supernatant, normalized to an OD_{260} of 2.0, was spotted
218 onto a polyethylenimine (PEI)-cellulose sheet (Merck) for thin layer chromatography
219 analysis (1.5 M KH_2PO_4 (pH 3.4)) (19). The TLC sheets were air dried, phosphor-
220 imaged, and (p)ppGpp spots were examined by densitometry as described before.
221

The identity of the spots was further confirmed by MALDI-TOF mass spectrometry.

Long-term survival Assay

Strains were cultured in MB7H9 media containing 0.02 % (w/v) glucose and 0.05 % (v/v) Tween 80 in the presence and absence of compounds (100 μM) of interest. The antibiotics were not used in the culture in order to rule out their effects on long-term survival. The colony forming units (cfu) were estimated at regular time intervals for 14 days. Bacterial cultures were vortexed with the 0.5 mm glass beads before plating on a MB7H9 agar plate for preventing the aggregation of cells.

Biofilm formation assay

For biofilm assay, *M. smegmatis* mc^2155 was grown in Sauton's media supplemented with 2% Glycerol and 0.05% Tween-80 and used as primary culture. The procedure was followed as illustrated elsewhere (20-23). Briefly, fully grown primary culture was washed with Sauton's media and then used as a secondary inoculum. Biofilm was cultured in six-well cell culture plate (Laxbro) in which primary inoculum was 100 times diluted with Sauton's medium. Inhibitors (100μg/mL) were added at zero time point. Culture plates were incubated in a humidified incubator set at 37 $^{\circ}$C and evaluated at different time points.

Mycobacterium tuberculosis Erdman biofilms were inoculated with stationary phase planktonic cultures into Sauton medium at a 1:100 dilution in 96-well plates to a final volume of 200 μl per well. Biofilm cultures were incubated in airtight plastic bags to restrict oxygen for 3 weeks, and then vented. Compounds were added to biofilm

cultures at the time of inoculation at the indicated concentrations. Photographs of biofilms were taken at the time indicated.

Biofilm Quantification

The biofilm formation was quantified in 96 well plates and the protocol was followed as described previously (23). Briefly, primary culture was washed and re-suspended in Sauton's medium to an optical density (O.D.) of 0.0025 at 590 nm. The inhibitors were added to the well containing 200 µL inoculum at zero time point and biofilm formation was monitored up to 144 h. The media was removed from the wells followed by washing with water. Subsequently, staining solution (1% crystal violet, 200 µL) was added to each well and the plate was incubated for 20 min. The wells were washed with water and dried. The dye was quantitated after solubilization in DMSO (200 µL) and consequently the absorption at 590 nm was recorded using a microplate reader. Experiment was performed in three biological replicates for each inhibitor.

Biofilm disruption assay

In this assay, *M smegmatis* mc^2155 strain was allowed to form biofilm in the Sauton's media in 6-well plate at 37°C humified incubator as described earlier. Inhibitors were administered below the biofilm at 72 hours time point by using one mL syringe. Biofilm growth was followed till 126 hours time point and plates were monitored for biofilm disruption. Experiment was conducted in three biological replicates

271 **Hemolysis Assay and Microscopy**

272 Hemolysis of human red blood cells (RBC) was monitored in the presence of synthetic
273 compounds. Left over blood sample obtained from Health Center, Indian Institute of
274 Science, Bangalore was used for this study. Hemolysis assay were performed as
275 described elsewhere (24). Briefly, blood sample was pelleted by centrifugation (500g,
276 10 min) and supernatant (plasma) was gently removed (treated with bleach and
277 discarded into biohazardous wastes). RBC pellet was washed and re-suspended in
278 phosphate buffer saline (PBS, pH 7.4). Assay was performed at varying concentration
279 of inhibitors (10 µl, 20-220 µg/mL) mixed with 190 µL diluted red blood cells (20
280 Dilution) in 96 well plate. 10 µL of 20 % SDS was used in positive control well and
281 10 µL of phosphate buffer was the negative control. Plate was incubated at 37 °C for
282 1 h. 100 µL of supernatant was transferred into eppendorf tubes and centrifugation for
283 10 minutes at 500 g. The supernatant was transferred into a fresh eppendorf tubes and
284 absorbance of the supernatant was measured at 540 nm in UV/Visible
285 spectrophotometer (Eppendorf). Experiment was performed in triplicates. RBCs treated
286 with synthetic compounds were observed under light microscope at 40X magnification.
287 Such RBC cells suspended in PBS were poured on slide, covered with cover slip,
288 cleaned and placed under the microscope.

289

290 **Cell culture**: Human lung epithelial cell line was cultured in Roswell Park Memorial
291 Institute (RPMI-1640) medium supplemented with 10% Fetal Bovine Serum (FBS).
292 The cultures were grown in humidified atmosphere with 5% CO_2 in incubator at 37°C
293 for 2-3 days. At nearly 80% confluency, the media was removed and cells were washed
294 with PBS and detached with 0.25% trypsin-EDTA at 37°C for 2-3 minutes.
295 Subsequently, 1 mL fresh media was added. Cells were pelleted down at 1000 rpm for 5

296 minutes and re-suspended in fresh medium (10 mL) in tissue culture flask. Cells were
297 mixed with trypan blue in 1:1 ratio and observed using haemocytometer under the
298 microscope in order to check the cell count.

299

300 **Cell permeability assay**: Cell suspension (nearly 2500 cells, 0.2ml) were added to each
301 well of 96-well plate and incubated for 24 hours for adherence. The culture media was
302 replaced with fresh media with compounds at concentration of 200 µg/ml. Cells were
303 incubated for 6 hours and media was removed, and cells were washed with PBS.
304 Adhered cells were removed using 0.25% trypsin-EDTA and cells were washed thrice
305 with PBS. Cell pellet was re-suspended in 50µl of PBS. Cells were lysed by heating at
306 95°C for 10 minutes followed by centrifugation at 15000 rpm for 10 minutes. Soup was
307 transferred to a labelled tube and consequently analyzed by mass spectrometry.

308

309 **Mass spectrometry**: MALDI was used for the peak identification of drugs. 1µl of cell
310 lysate mixed with 1µl CCA was spotted on plate and allowed to dry. Mass spectra were
311 recorded on Ultraflex II MALDI-TOF/TOF mass spectrometer equipped with a
312 smartbeam™ (Bruker Daltonik, Germany) operated in positive-ion, reflectron mode.
313 Three to five mass spectra were averaged for each individual sample using 1000–1500
314 laser shots each over the entire spot on the MALDI target plate PBS wash was taken as
315 the negative control.

316

317 **MTT assay**: The effect of inhibitors on cell viability was studied using MTT assay.
318 It is a colorimetric assay, which measures the metabolic activity of the cell as a function
319 of reduction of tetrazolium dye to insoluble formazon. H460 cell lines were used to

320 determine the cytotoxicity. Cell suspension (nearly 2500 cell, 0.2ml) were seeded in 96
321 well plate and incubated for 24 hours for the cells to adhere. After that culture, media
322 was replaced with fresh media with the inhibitors in the concentration range of 100-500
323 µg/ml. Experiment was conducted in three biological replicates for each concentration
324 of the inhibitor. After 36 hours of incubation, 20 µl of MTT at the concentration of
325 0.5mg/ml was added to each well followed by incubation for 4 hours. Later, media was
326 removed and cells were washed with PBS. 100 µl of Dimethylsulphoxide (DMSO) was
327 used to dissolve the formazon crystal followed by measuring absorbance at 570 nm
328 using ELISA plate reader. Media alone and media with cells (without inhibitor) were
329 used as controls. The percentage of cell survival was calculated using the following
330 formula:

331 Cell survival (%) = (AbsorbanceTreatment/AbsorbanceControl) X 100

332

333

334

335

336

337

338

339

340

Results

Synthesis

The amino group at the *C*-2 substituent of the guanine moiety in guanosine was modified with benzoyl and acetyl groups. 2', 3' and 5' positions were protected through acetylation.

Synthesis of protected guanosine derivative **1** and **3** were conducted as shown in **Scheme 1** (Figure 2). Per-acetylation of guanosine using acetic anhydride in pyridine afforded acetyl protected guanosine derivative **1**, in 56% yield. Incorporation of acetyl moiety at the available hydroxyl and amine sites was verified through physical techniques. The –N*H* proton in **1** resonated at 10.47 ppm as a singlet in ^{1}H NMR spectrum, whereas anomeric carbon in **1** resonated at 87.2 ppm in ^{13}C NMR spectrum. Peaks at 169.4-172.9 ppm corresponded to carbonyl moieties of ester and amide functionalities in **1**. The molecular ion peak in **1** was observed at 451.97 [M] in MALDI-TOF mass spectrum, as the base peak (Figure 3).

<Figure 2>

Similarly, benzoylation of guanosine using benzoyl chloride in pyridine led to the formation of benzoyl protected guanosine intermediate **2**, in 62% yield. *O*-Debenzoylation of **2**, by treatment with NaOH (0.1 M) in MeOH, followed by *O*-acetylation using acetic anhydride in pyridine, afforded protected guanosine **3**, in 41% yield (**Scheme 1,** Figure 2). The formation of **3** was confirmed by NMR spectroscopy and mass spectrometry. In the MALDI-TOF mass spectrum, the appearance of peak at 513.8 [M] and 536.04 $[M + Na]^{+}$, as the base peak, corresponded to the molecular ion peak of **3** (Figure 3). The -N*H* proton appeared as a broad singlet at 9.46 ppm in ^{1}H

NMR spectrum, attributed to benzoyl amide functionality of **3**. In ^{13}C NMR spectrum of **3**, anomeric carbon appeared at 87.3 ppm, whereas carbonyl groups of ester functionalities resonated in the region of 169.9 to 171.0 ppm.

<Figure 3>

<Figure 4>

AB and AC compounds inhibited the *in-vitro* and *in-vivo* Rel activity

In-vitro activity assays were performed in the presence of 100 µM acetylated compound (AC compound) and acetylated benzoylated compound (AB compound). At 100 µM concentration, AC and AB compounds inhibited pppGpp synthesis by ~30% and ~75 %, respectively (Figure 4). The IC_{50} value was calculated to be nearly 40 micromolar by testing the inhibition in presence of different doses of acetylated benzoylated compounds (Figure 4b).

Next, we studied the effects of compounds on bacterial cells in minimal media conditions and quantitated the *in-vivo* (p)ppGpp levels in treated *M. smegmatis* cells in comparison to the untreated cells. The synthetic compounds inhibited (p)ppGpp synthesis in *M. smegmatis.* Densitometric analysis was done to check the decrease in (p)ppGpp levels by the application of Image J software. A significant decrease in (p)ppGpp levels was observed as determined by t-test (Figure 5). The AB compound was found to be more potent in inhibiting the *in-vivo* (p)ppGpp synthesis.

<Figure 5>

Previously, it has been reported that the mycobacterial cells devoid of the *rel* gene are morphologically different and elongated (25-26). We analyzed the average length of the *M. smegmatis* cells treated with AB compound and found them to be elongated (Figure S6), which supports alterations in (p)ppGpp levels, indirectly.

Binding Kinetics by Isothermal Titration Calorimetry

We did isothermal titration calorimetry based experiment to confirm specific binding of the AB compound to the Rel molecule. From the ITC curve of the Rel enzyme from *M. smegmatis* with the AB compound in a range of concentrations, a dissociation constant as ~10 μM (Figure 6) was obtained. The binding was predominantly driven by enthalpy. The n value obtained was 1, signifying one binding site of AB compound on the Rel enzyme (Figure 6).

<Figure 6>

Enzyme kinetics of Rel

Enzyme kinetics for (p)ppGpp synthesis by Rel_{Msm} (Full length Rel enzyme from *M. smegmatis*) in the presence of 100 μM of AC and AB compounds were followed to understand the level of inhibition in comparison to that of the Rel control. Substrate concentrations were varied from 0-2000 μM for the kinetics study of Rel in the presence of AC compound. For the AB compound, 0-3000 μM range of substrate

concentration was used as higher concentration of substrate was required for achieving saturation. Enzyme kinetics curve was observed to fit with Hill equation.

<Figure 7>

The $K_{0.5}$ was found to increase with the concomitant reduction in the Vmax value in the presence of AB compound. Such changes in the $K_{0.5}$ and Vmax values indicate mixed inhibition (Figure 7). We observed that the AC compound lead to an increase in the $K_{0.5}$ value, without significant change in the Vmax value, suggesting competitive inhibition. The Hill coefficient value was observed to be more than one (>1) indicating positive cooperative binding where binding of one ligand molecule to the enzyme induces the binding of other ligand molecules.

Synthetic compounds affect cell survival

(p)ppGpp synthesis is important for long term survival of mycobacteria (27).Therefore, we were intrigued to look for the effects of the synthetic compounds on *M. smegmatis* survival. We found significant inhibition of long-term survival in the presence of the compounds (100 μM) in comparison to the wild-type untreated controls (Figure 8). Both AC and AB compounds showed considerable inhibition. A Rel knockout strain was used as a control which also showed the decreased long term survival as reported by others (25). We used the Rel complemented knock out strain and found that long-term survival was restored only in the absence of compounds.

<Figure 8>

The Rel KO did not show further inhibition of long-term survival in the presence of the compounds (Figure 8), supporting that Rel was the target of the compounds. Our compounds target Rel and inhibit (p)ppGpp synthesis, thereby affecting long term survival in *M. smegmatis*.

Biofilm formation and quantification

Bacterial adaptation to hostile conditions involves activation of cascades and transitions to resilient phenotypes such as from planktonic to biofilm forms. Biofilms protect the bacteria from stress and induce tolerance to antibiotics. Biofilms are made up of microbial populations enclosed in a matrix. Biofilms are a thousand times more tolerant to antibiotics in comparison to the planktonic cells (11). It has been shown that tuberculosis bacteria incapable of forming biofilms cannot survive inside the host (27). Recent evidences indicate that *M. tuberculosis* display a biofilm-like phenotype during infection that could help it survive inside the host (28). Alarmone molecule (p)ppGpp has been directly linked to biofilm formation. It has been shown that *M. tuberculosis* and *M. smegmatis rel* knock out strains are not effective in forming biofilms (10-11). Therefore, (p)ppGpp formation and its associated pathways are seen as an important drug target for biofilm inhibition (29-30).

We analyzed biofilm formation in *M. smegmatis* in the presence of synthetic compounds at 100 μg/mL. A representative picture of biofilm formation is shown in Figure 9.

<Figure 9>

<Figure 10>

We also did the quantification of biofilm in *M. smegmatis* in the presence and absence of the synthetic compounds in comparison to the appropriate controls at different time points (up to 144 hours, Figure 10). The biofilm was quantified by crystal violet assay (31). In order to determine whether compounds can disrupt already formed biofilms, biofilm disruption assays were performed where compounds were added just below the biofilm with the application of a 1 mL syringe after 72 hours of growth. We assessed the change in biofilm morphology after 54 hours of addition of the compound in comparison to the control (Figure S7). The AB and AC compounds were found to inhibit the formation of biofilms as well as disrupt the pre-formed biofilms in *M. smegmatis*. It should be mentioned here that both compounds were not bacteriocidal in *Mycobacterium smegmatis* as determined by the cfu (colony forming unit) assay. In this assay, bacteria were cultured in the presence of the synthesized compounds. The bacterial cells from early log phase were plated over the LB agar. We could not find a significant difference as determined by the student t-test in cfu of treated cells in comparison to the untreated cells.

Subsequently, the effect of the compounds on biofilm formation by *M. tuberculosis* was examined and inhibition was observed suggesting reproducibility of compound effects in the different mycobacterial species and possible clinical relevance (Figure 9).

Toxicity: Hemolysis assay and Microscopic studies

The effect of synthetic compounds on normal RBC healthy cells and their toxicities were evaluated. The compounds (at 220 µg/mL) were found to be non-toxic and results

489 were comparable with the negative controls as presented in figure S8. Healthy RBCs
490 are biconcave in shape. So, treated RBC cells were analyzed under a microscope for
491 visualizing morphological changes, if any. RBCs treated with the synthetic compounds
492 were observed to be biconcave (Figure S8).
493
494 **Compounds were permeable to human lung epithelial cell line**

495 Permeability of compounds was tested using mass spectrometry for studying the drug
496 permeability across the cell membrane. Cells were treated with compounds and the cell
497 lysates were analyzed using MALDI. The peaks corresponding to the compounds were
498 absent in control and present in the treated sample. Experiment was done in three
499 biological replicates to confirm the observation. Here, cells were washed with PBS
500 (three times) before lysis in order to prevent any carry forward of the inhibitor present
501 outside the cell. Compounds were not detected in final PBS wash (32).
502
503 **MTT toxicity assay**

504 We performed an MTT assay to check the cell cytotoxicity in presence of the inhibitors.
505 Here, cells with media were taken as the control and compared with the sample (cell +
506 media + compound) incubated for 36 hours. 100-500µg/mL and 100-400µg/mL range
507 of concentrations were tested for the acetylated and acetylated benzoylated compounds,
508 respectively. No cytotoxicity was observed for the treated samples and they were
509 comparable to the control (Figure 11). Percentage survival was calculated to be more
510 than 95% upto the concentration of 400 µg/mL for both tested compounds.
511
512 **<Figure 11>**

Discussion

Unlike exponential phase, the stationary phase of bacteria is characterized by low rate of translation, transcription and replication (33). Therefore, many antibiotics that target these pathways are virtually ineffective in the stationary phase. Further, bacteria exposed to hostile conditions like nutritional starvation and other kinds of stresses induce the stringent response, which is mediated by (p)ppGpp and helps the bacteria survive under such conditions (11). The antimicrobials that target stress induced stringent response pathways are very few, thus such an approach offers a unique possibility (34).

(p)ppGpp analogues such as Relacin have been shown to be effective in inhibiting ppGpp synthesis, stress responses, and key survival processes like sporulation (13). In the latter study, it has been indicated that the isobutyryl group at second position of guanine is critical for inhibition. We substituted it to the bulkier benzoyl group as well as to the smaller acetyl group. We found benzoyl group to be better substituent for inhibition. Based on docking studies, we found benzoyl ring at C-2 position of the guanine base to be involved in stacking interaction with lysine residue at position 251 of Rel enzyme from *Streptococcus equisimilis* (Figure 12). The latter lysine residue was found to be conserved in Rel enzyme from mycobacteria (Figure S9).

<Figure 12>

In this study, we have shown that (p)ppGpp analogs can be used to inhibit (p)ppGpp synthesis in acid fast bacterium such as Mycobacteria. Earlier, biofilm

formation has been shown to be defective in a Rel mutant strain of *M. smegmatis* and bacterial cells were found to be elongated (26). Expectedly, cells treated with compounds used here were not able to form biofilm and were elongated, consistent with the studies in Rel mutant (26). The long treatment regime, antibiotic tolerance and the emergence of multiple drug resistance in *M. tuberculosis* are attributed to its stress response (27). It is now well-known that the bacterial strains with defective (p)ppGpp synthesis are metabolically compromised (1). Recent studies have suggested that the inhibition of (p)ppGpp production would have a detrimental effect on bacterial survival and virulence (10). The inhibition of the stringent response appears to be a promising approach to control pathogens, such as *M. tuberculosis*, the causative agent of tuberculosis, which is also known to persist inside the host. We observed that compounds were non-toxic as demonstrated by MTT assay and RBC hemolysis assay. Also, compounds were found to be permeable to the cell membranes as evident by the detection of synthetic compounds in cell lysates by mass spectrometry.

We followed enzyme kinetics for Rel from *M. smegmatis* and interestingly observed it to fit as per Hill equation. Although the inhibition exhibited by these compounds is in the micromolar range, they present a novel strategy, in which the stress response of one of the most persistent pathogens, *M. tuberculosis*, can be potentially targeted. In the future, these compounds will be further improved by modifications in order to achieve the inhibition in nanomolar range and consequently evaluated for their use in humans.

Acknowledgement

Authors acknowledge Proteomics facility, Molecular Biophysics Unit, Indian Institute of Science, Bangalore and NMR facility, Department of Organic Chemistry, Indian Institute of Science, Bangalore, for the help with the characterization of the compounds.

Funding

KS acknowledges research associateship from Indian Institute of Science, Bangalore, India. K.F. is supported by a pilot award from the Center for Women's Infectious Disease Research (cWIDR) at Washington University School of Medicine. NB acknowledges Department of Biotechnology, Government of India for the research fellowship. KGM acknowledges CSIR, New Delhi for the fellowship. NJ acknowledges Department of Science and Technology, Government of India for funding the laboratory. C.L.S. is supported by a Beckman Young Investigator Award from the Arnold and Mabel Beckman Foundation, an Interdisciplinary Research Initiative grant from the Children's Discovery Institute of Washington University and St. Louis Children's Hospital, and NIH grant 4R33AI111696. DC acknowledges Centre of Excellence grant, Department of Biotechnology, Government of India for funding the laboratory.

Conflict of Interest

None to declare.

586 **Reference:**

587 1. **Liu K, Bittner AN, Wang JD.** 2015. Diversity in (p)ppGpp metabolism and
588 effectors. Curr Opin Microbiol **24:**72-79.

589 2. **Liu K, Myers AR, Pisithkul T, Claas KR, Satyshur KA, Amador-Noguez D,**
590 **Keck JL, Wang JD.** 2015. Molecular mechanism and evolution of guanylate
591 kinase regulation by (p)ppGpp. Mol Cell **57:**735-749.

592 3. **Hauryliuk V, Atkinson GC, Murakami KS, Tenson T, Gerdes K.** 2015.
593 Recent functional insights into the role of (p)ppGpp in bacterial physiology. Nat
594 Rev Microbiol **13:**298-309.

595 4. **Dahl JL, Arora K, Boshoff HI, Whiteford DC, Pacheco SA, Walsh OJ, Lau-**
596 **Bonilla D, Davis WB, Garza AG.** 2005. The relA homolog of Mycobacterium
597 smegmatis affects cell appearance, viability, and gene expression. J Bacteriol
598 **187:**2439-2447.

599 5. **Kriel A, Bittner AN, Kim SH, Liu K, Tehranchi AK, Zou WY, Rendon S,**
600 **Chen R, Tu BP, Wang JD.** 2012. Direct regulation of GTP homeostasis by
601 (p)ppGpp: a critical component of viability and stress resistance. Mol Cell
602 **48:**231-241.

603 6. **Klinkenberg LG, Lee JH, Bishai WR, Karakousis PC.** 2010. The stringent
604 response is required for full virulence of Mycobacterium tuberculosis in guinea
605 pigs. J Infect Dis **202:**1397-1404.

606 7. **Chatterji D, Ojha AK.** 2001. Revisiting the stringent response, ppGpp and
607 starvation signaling. Curr Opin Microbiol **4:**160-165.

608 8. **Dahl JL, Kraus CN, Boshoff HI, Doan B, Foley K, Avarbock D, Kaplan G,**
609 **Mizrahi V, Rubin H, Barry CE, 3rd.** 2003. The role of RelMtb-mediated
610 adaptation to stationary phase in long-term persistence of Mycobacterium
611 tuberculosis in mice. Proc Natl Acad Sci U S A **100:**10026-10031.

612 9. **Klinkenberg LG, Lee J-H, Bishai WR, Karakousis PC.** 2010. The stringent
613 response is required for full virulence of Mycobacterium tuberculosis in guinea
614 pigs. The Journal of infectious diseases **202:**1397-1404.

615 10. **Weiss LA, Stallings CL.** 2013. Essential roles for Mycobacterium tuberculosis
616 Rel beyond the production of (p)ppGpp. J Bacteriol **195:**5629-5638.

617 11. **Syal K, Maiti K, Naresh K, Chatterji D, Jayaraman N.** 2015. Synthetic
618 glycolipids and (p)ppGpp analogs: development of inhibitors for mycobacterial
619 growth, biofilm and stringent response. Adv Exp Med Biol **842:**309-327.

620 12. **Syal K, Bhardwaj N, Chatterji D.** 2017. Vitamin C targets (p)ppGpp synthesis
621 leading to stalling of long-term survival and biofilm formation in
622 Mycobacterium smegmatis. FEMS Microbiology Letters **364:**fnw282-fnw282.

623 13. **Wexselblatt E, Oppenheimer-Shaanan Y, Kaspy I, London N, Schueler-**
624 **Furman O, Yavin E, Glaser G, Katzhendler J, Ben-Yehuda S.** 2012.
625 Relacin, a novel antibacterial agent targeting the Stringent Response. PLoS
626 Pathog **8:**e1002925.

627 14. **Wexselblatt E, Kaspy I, Glaser G, Katzhendler J, Yavin E.** 2013. Design,
628 synthesis and structure-activity relationship of novel Relacin analogs as
629 inhibitors of Rel proteins. Eur J Med Chem **70:**497-504.

630 15. **Syal K, Tadala R.** 2015. Modifications in trypsin digestion protocol for
631 increasing the efficiency and coverage. Protein Pept Lett **22:**372-378.

632 16. **Jain V, Saleem-Batcha R, Chatterji D.** 2007. Synthesis and hydrolysis of
633 pppGpp in mycobacteria: A ligand mediated conformational switch in Rel.
634 Biophysical Chemistry **127:**41-50.

635 17. **Syal K, Chatterji D.** 2015. Differential binding of ppGpp and pppGpp to E.
636 coli RNA polymerase: photo-labeling and mass spectral studies. Genes Cells
637 **20:**1006-1016.

638 18. **Syal K, Joshi H, Chatterji D, Jain V.** 2015. Novel pppGpp binding site at the
639 C-terminal region of the Rel enzyme from Mycobacterium smegmatis. FEBS J
640 **282:**3773-3785.

641 19. **Murdeshwar MS, Chatterji D.** 2012. MS_RHII-RSD, a dual-function RNase
642 HII-(p)ppGpp synthetase from Mycobacterium smegmatis. J Bacteriol
643 **194:**4003-4014.

644 20. **Naresh K, Bharati BK, Avaji PG, Chatterji D, Jayaraman N.** 2011.
645 Synthesis, biological studies of linear and branched arabinofuranoside-
646 containing glycolipids and their interaction with surfactant protein A.
647 Glycobiology **21:**1237-1254.

648 21. **Naresh K, Bharati BK, Avaji PG, Jayaraman N, Chatterji D.** 2010.
649 Synthetic arabinomannan glycolipids and their effects on growth and motility of
650 the Mycobacterium smegmatis. Org Biomol Chem **8:**592-599.

651 22. **Naresh K, Bharati BK, Jayaraman N, Chatterji D.** 2008. Synthesis and
652 mycobacterial growth inhibition activities of bivalent and monovalent
653 arabinofuranoside containing alkyl glycosides. Org Biomol Chem **6:**2388-2393.

654 23. **Mathew R, Mukherjee R, Balachandar R, Chatterji D.** 2006. Deletion of the
655 rpoZ gene, encoding the omega subunit of RNA polymerase, results in
656 pleiotropic surface-related phenotypes in Mycobacterium smegmatis.
657 Microbiology **152:**1741-1750.

658 24. **Syal K, Maiti K, Naresh K, Avaji PG, Chatterji D, Jayaraman N.** 2016.
659 Synthetic arabinomannan glycolipids impede mycobacterial growth, sliding
660 motility and biofilm structure. Glycoconjugate Journal **33:**763-777.

661 25. **Dahl JL, Arora K, Boshoff HI, Whiteford DC, Pacheco SA, Walsh OJ, Lau-**
662 **Bonilla D, Davis WB, Garza AG.** 2005. The relA Homolog of Mycobacterium
663 smegmatis Affects Cell Appearance, Viability, and Gene Expression. Journal of
664 Bacteriology **187:**2439-2447.

665 26. **Gupta KR, Baloni P, Indi SS, Chatterji D.** 2016. Regulation of Growth, Cell
666 Shape, Cell Division, and Gene Expression by Second Messengers (p)ppGpp
667 and Cyclic Di-GMP in Mycobacterium smegmatis. J Bacteriol **198:**1414-1422.

668 27. **Primm TP, Andersen SJ, Mizrahi V, Avarbock D, Rubin H, Barry CE, 3rd.**
669 2000. The stringent response of Mycobacterium tuberculosis is required for
670 long-term survival. J Bacteriol **182:**4889-4898.

671 28. **Islam MS, Richards JP, Ojha AK.** 2012. Targeting drug tolerance in
672 mycobacteria: a perspective from mycobacterial biofilms. Expert Rev Anti
673 Infect Ther **10:**1055-1066.

674 29. **de la Fuente-Nunez C, Reffuveille F, Haney EF, Straus SK, Hancock RE.**
675 2014. Broad-spectrum anti-biofilm peptide that targets a cellular stress response.
676 PLoS Pathog **10:**e1004152.

677 30. **Nunes-Alves C.** 2014. Biofilms: Targeting (p)ppGpp disrupts biofilms. Nat Rev
678 Micro **12:**461-461.

679 31. **O'Toole GA, Kolter R.** 1998. Initiation of biofilm formation in Pseudomonas
680 fluorescens WCS365 proceeds via multiple, convergent signalling pathways: a
681 genetic analysis. Mol Microbiol **28:**449-461.

682 32. **Elmquist A, Langel U.** 2003. In vitro uptake and stability study of pVEC and
683 its all-D analog. Biol Chem **384:**387-393.

684 33. **Nazir A, Harinarayanan R.** 2016. (p)ppGpp and the bacterial cell cycle. J
685 Biosci **41:**277-282.

686 34. **Andresen L, Varik V, Tozawa Y, Jimmy S, Lindberg S, Tenson T,**
687 **Hauryliuk V.** 2016. Auxotrophy-based High Throughput Screening assay for
688 the identification of Bacillus subtilis stringent response inhibitors. Sci Rep
689 **6:**35824.

690

691

Figure Legends

Figure 1. Structure of pppGpp and Relacin.

Figure 2. *Reagents and conditions:* (i) Acetic anhydride, 4-dimethylaminopyridine, pyridine, 0 ^{o}C-rt, 12 h, 56%. (ii) Benzoyl chloride, 4-dimethylaminopyridine, pyridine, 0 ^{o}C-rt, 12 h, 62%.(iii) a. Sodium hydroxide (2 M), methanol, rt, 12 h; b. Acetic anhydride, 4-dimethylaminopyridine, pyridine, 0 ^{o}C-rt, 12 h, 41% (after two steps). In the text, compound 1 is referred as acetylated compound or AC compound and compound 3 is referred as acetylated benzoylated compound or AB compound, respectively.

Figure 3. Upper Panel- MALDI-TOF analysis of acetylated compound (AC Compound). 451.9 m/z value correspond to the acetylated derivative of guanosine (AC compound). **Lower Panel**- MALDI-TOF analysis of acetylated benzoylated guanosine (AB compound). 513.8 m/z value corresponds to the mass of acetylated benzoylated compound and 536.0 m/z value is its sodiated adduct.

Figure 4A. Inhibitory effects of AC and AB compounds on *in-vitro* pppGpp synthesis at 100 µM concentration. Experiment was done in three biological replicates. Densitometric analysis was performed and values obtained were normalized with respect to wildtype (WT or 4). Student t-test was carried out to confirm the significance. P-value was less than 0.05 in the case of 6 and 7. **4B.** Dose dependent inhibition of *in-vitro* pppGpp synthesis ranging from 1 to 250 µM.

Figure 5. *In-vivo* estimation of (p)ppGpp levels in *M. smegmatis.* Experiment has been conducted in three biological replicates. Student t-test was performed to confirm the significance. P- value was found to be less than 0.05 for both AC compound and BC compound.

Figure 6. Binding of the acetylated benzoylated compound to Rel enzyme from *M. smegmatis*. Isothermal titration calorimetry curve corresponding to the binding of the synthetic compound to Rel enzyme at 25 °C is presented here. Upper panel showed the raw data for the titration of Rel enzyme with AB compound and the lower panel

722 indicated the integrated heat of binding obtained from the raw data. Model for one site
723 binding was implicated for fitting the curve. The 'n' represents the number of binding
724 site that is one and the K represents the association constant (K_a). The dissociation
725 constant, K_d, can be calculated by reciprocating K_a and was calculated to be nearly 10
726 µM.

727 **Figure 7.** Enzyme kinetics of $Rel_{Msm.}$ The rate of formation of ppGpp as a function of
728 substrate GTP is shown here. (a) shows the formation of product with varying substrate
729 concentrations and (b) shows the phosphorimage data of the same. Table below
730 quantifies $K_{0.5}$ and Vmax of the reaction in the absence and presence of the synthesized
731 inhibitors. –ve- Negative control (assay buffer); WT- control where inhibitor was not
732 added; Other lanes- Assay mixture with increasing concentration of GTP. The
733 concentration of the protein (Rel_{Msm}) was kept at 200µg/mL. Student t-test was
734 performed to analyze the significant change in Vmax and $K_{0.5}$ values. Graph was fitted
735 with Hill equation. The Hill coefficient value was found to be 1.89 ± 0.17.

736 **Figure 8.** Long term survival in presence and absence of the synthetic compounds
737 (100µM) with Rel Knock out (KO) and Rel Complement controls in triplicates.
738 Experiment has been performed in three biological replicates. Inhibition was found to
739 be significant for both AB and AC compounds.

740 **Figure 9.** Biofilm formation in the presence of AC and AB compounds (100µg/mL) in
741 comparison with control experiment where compound was not added in *M. tuberculosis*
742 and *M. smegmatis*.

743 **Figure 10.** Biofilm quantification assay in the presence of compounds (100µg/mL) in
744 Sauton's media in three biological replicates. Biofilm formation was found to be
745 decreased in the treated bacterial cells. Compounds were added at zero time point.

746 **Figure 11.** MTT assay results in presence of range of concentration of synthetic
747 compounds using H460 cell line. X-axis: Concentration of Compound; Y-axis:
748 Absorbance at 570nm. A) Acetylated benzoylated compound, B) Acetylated
749 Compound.

750 **Figure 12.** The crystal structure of Relseq385, Rel/Spo from *Streptococcus equisimilis,*
751 was utilized for *insilico* docking. GDP molecule was removed from the active site of

752 the protein structure. The acetylated benzoylated compound structure (in low energy
753 state) was positioned at the active site in place of GDP and all of the rotatable bonds
754 were kept flexible. (A) Two dimensional representation of the interactions at the active
755 site. Red line indicates stacking interaction whereas purple dotted line shows hydrogen
756 bonding. B) Three dimensional depiction of the active site with bound acetylated
757 benzoylated compound.

758

759

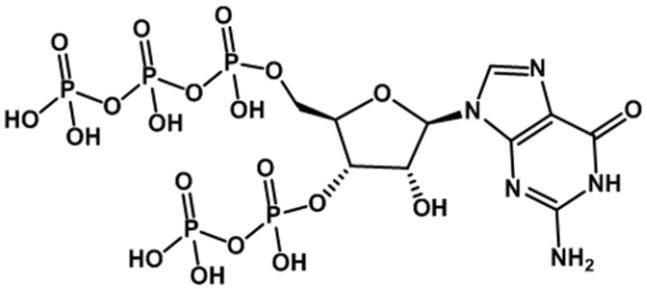

pppGpp

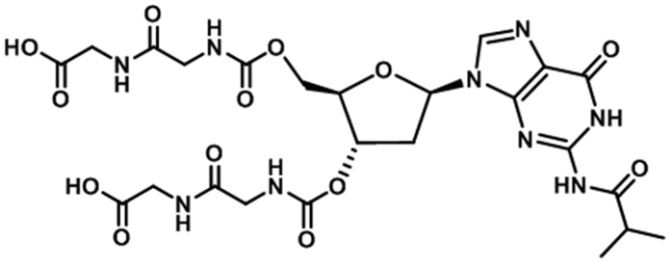

Relacin

Scheme 1

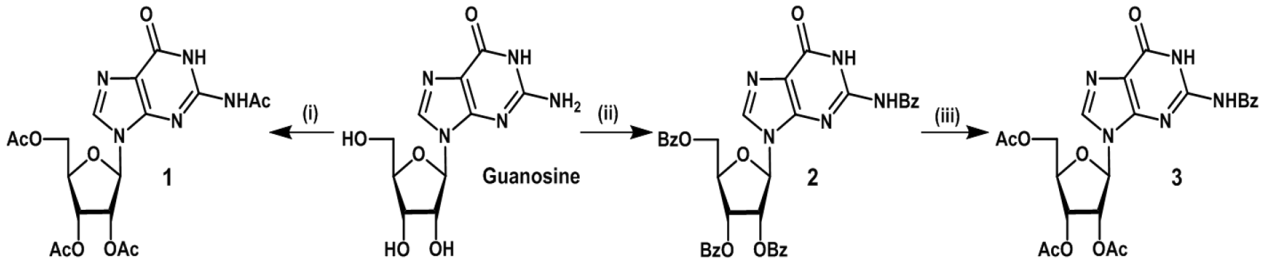

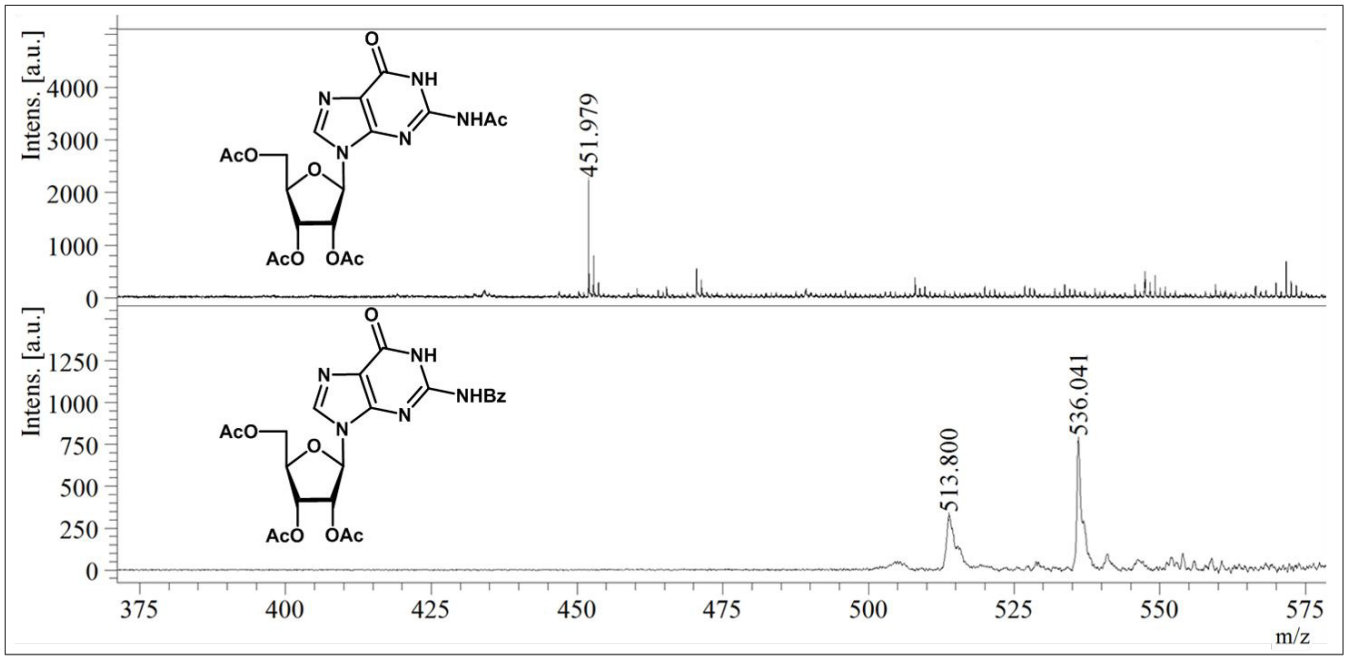

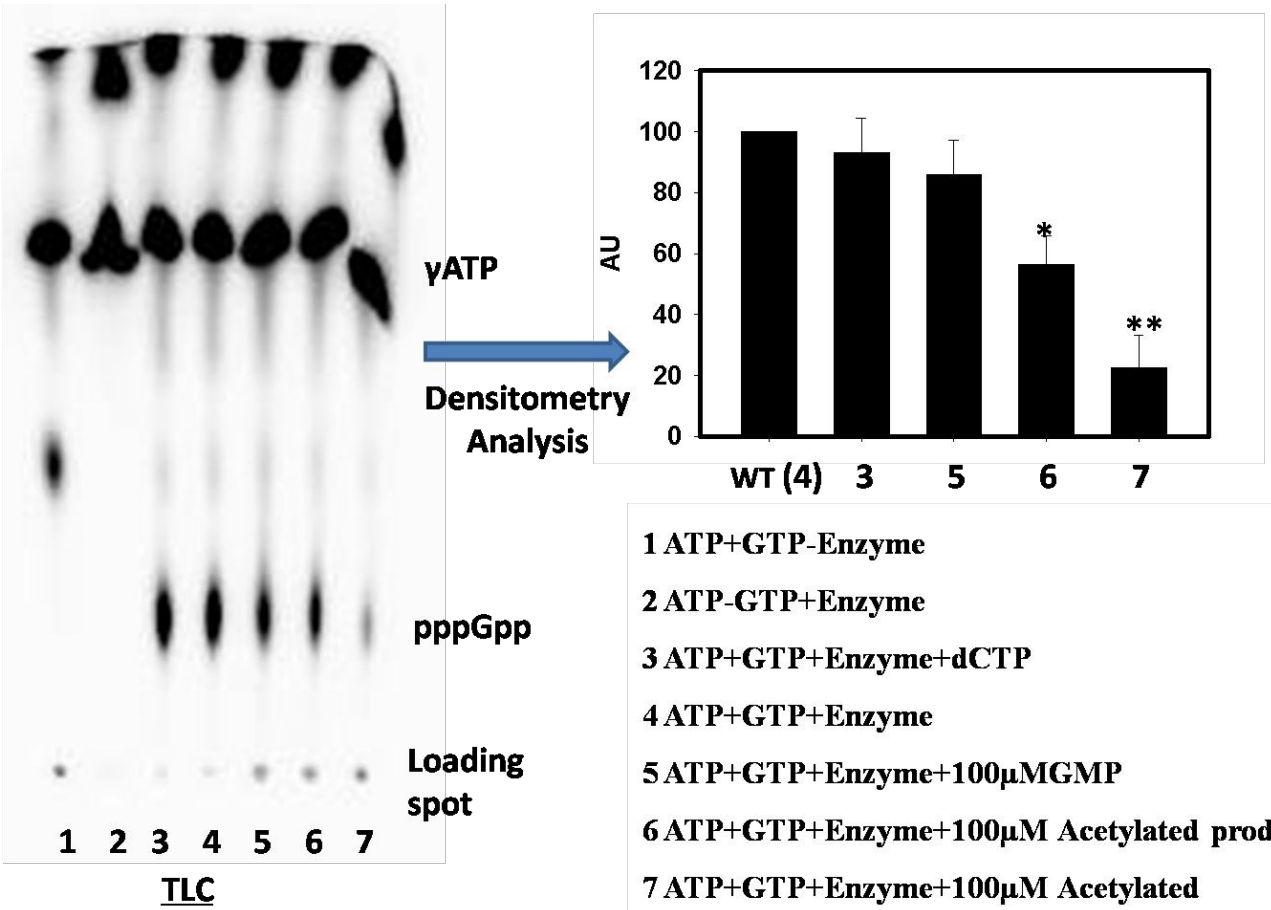

1 ATP+GTP-Enzyme

2 ATP-GTP+Enzyme

3 ATP+GTP+Enzyme+dCTP

4 ATP+GTP+Enzyme

5 ATP+GTP+Enzyme+100μMGMP

6 ATP+GTP+Enzyme+100μM Acetylated product.

7 ATP+GTP+Enzyme+100μM Acetylated Benzoylated product

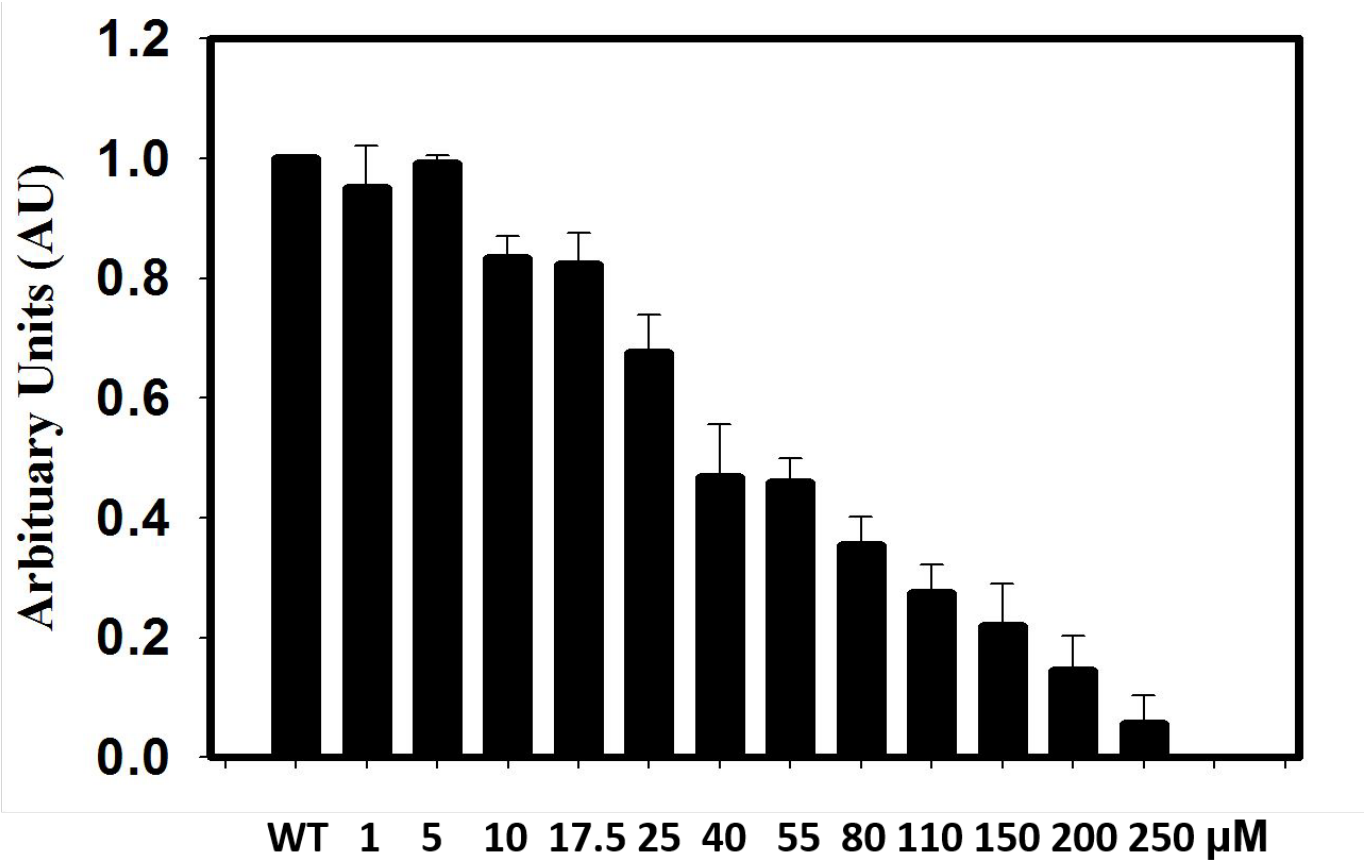

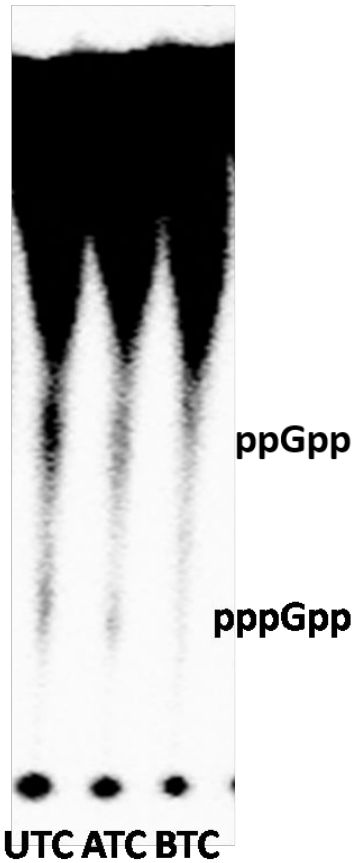

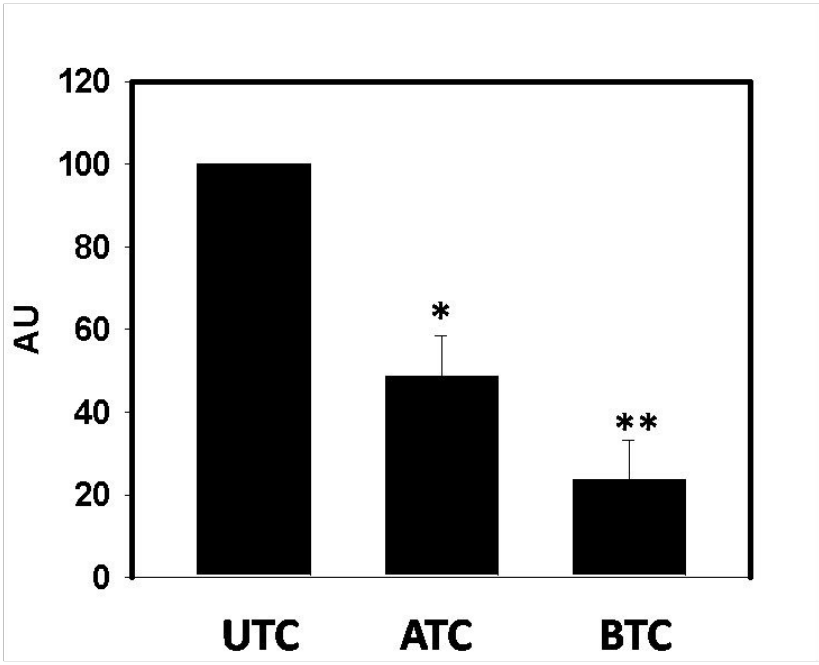

UTC Untreated cells
ATC Acetylated compound treated cells
BTC Acetylated Benzoylated compound treated cells

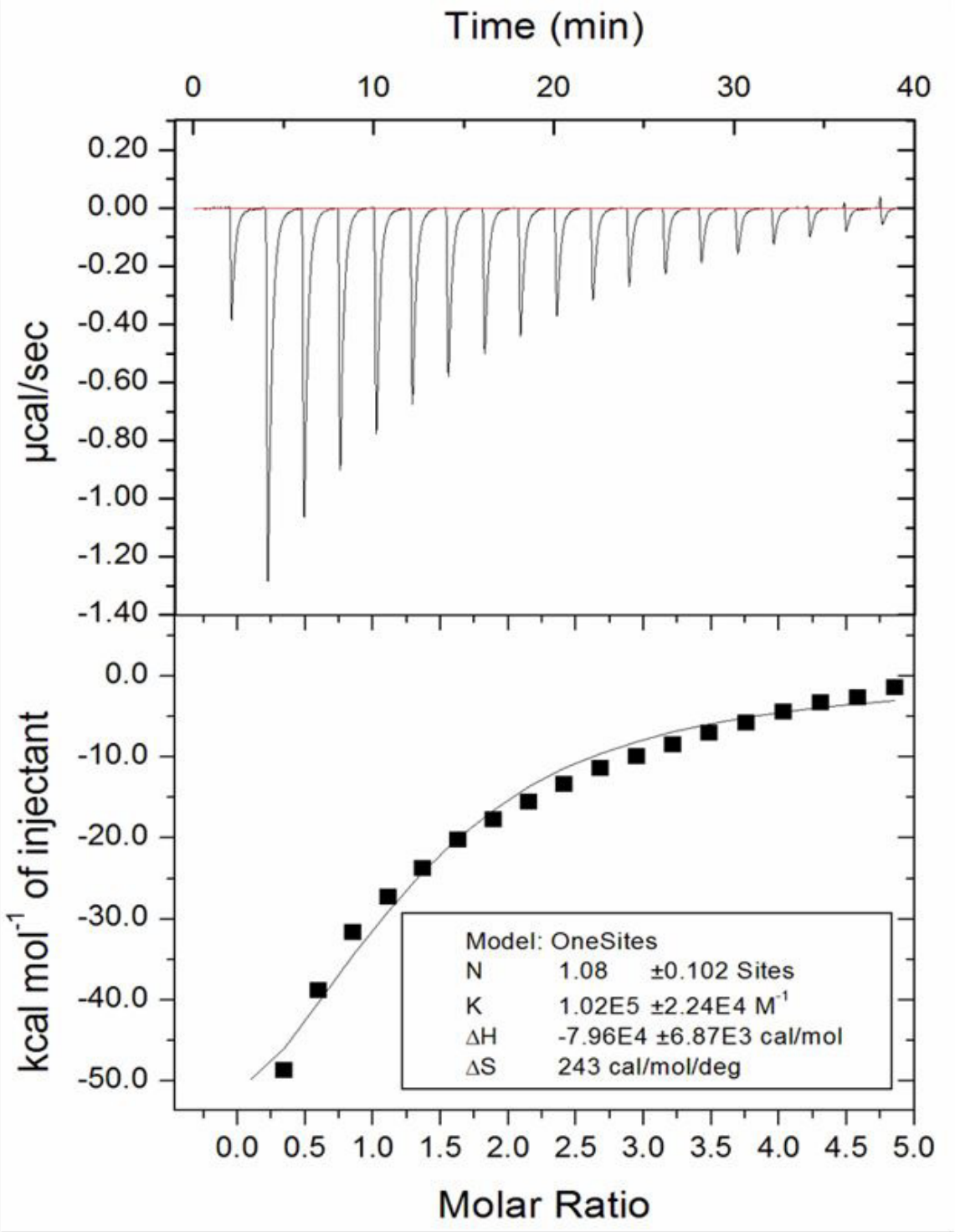

a)

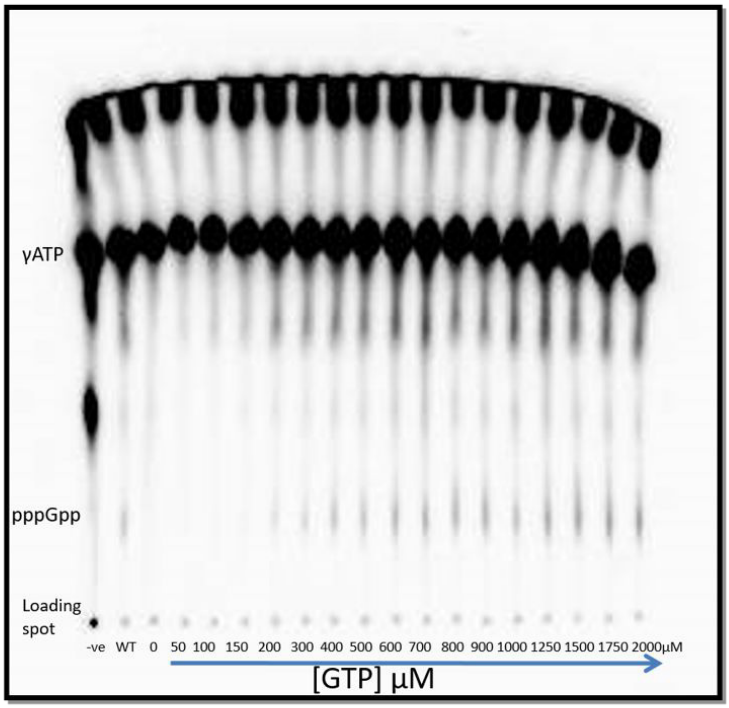

b)

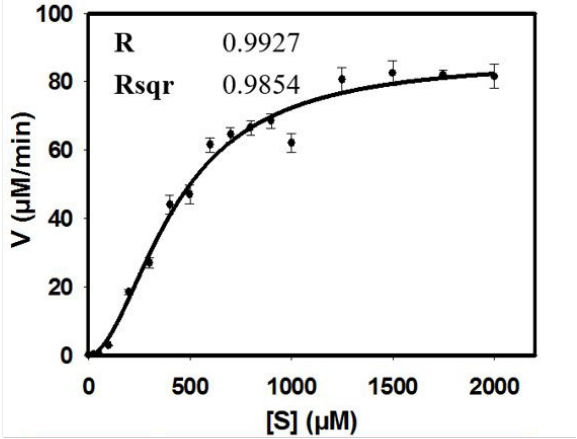

	$K_{0.5}$ (μM)	Vmax (μM/min)
Rel WT	425.2±22.2	86.7±2.86
With AB Compound (100μM)	1201±67.5	35±1.5
With AC Compound (100μM)	920±64.4	94.3±14.7